PHYSICAL REVIEW B **73**, 041401(R) (2006)

Second-harmonic generation from arrays of symmetric gold nanoparticles

M. D. McMahon, R. Lopez, and R. F. Haglund, Jr.
Department of Physics and Astronomy and Institute for Nanoscale Science and Engineering, Vanderbilt University, Nashville, Tennessee 37235, USA

E. A. Ray and P. H. Bunton
Department of Physics and Mathematics, William Jewell College, Liberty, Missouri 64068, USA
(Received 10 November 2005; published 11 January 2006)

We show that second-harmonic light can be generated from a diffraction grating of gold nanoparticles with planar inversion symmetry. By measuring the angular distribution of second-harmonic light, we observe an effect in which the diffraction pattern of the grating is superimposed on the intrinsic second-harmonic radiation pattern of the nanoparticles. This result suggests that the second-harmonic generation may be used to study coherent nonlinear optical effects in symmetric as well as asymmetric metal nanoparticles.

DOI: 10.1103/PhysRevB.73.041401 PACS number(s): 78.67.Bf, 42.65.Ky, 42.25.Fx

Second-harmonic generation (SHG) has been used for over two decades as an optical probe of electronic properties of metal nanoparticles (NPs) of varying shape, size, composition, and spatial organization.[1–11] The objectives of metal NP studies, in general, have ranged from measuring electron dephasing,[1,4,12–16] to pinpointing the origin of surface-enhanced Raman scattering[2,17–19] and assessing the potential for plasmonic applications such as all-optical switching.[20–23]

It is usually taken for granted that symmetry forbids the generation of second-harmonic light in centrosymmetric NP systems.[24] Even when asymmetric NPs are arranged so that the *overall* array has inversion symmetry, SHG is completely suppressed along the illumination direction.[16] This quenching of SHG along the illumination direction holds true for both surface and bulk SHG contributions;[3,15,16] for this reason, the potential of SHG for probing electron dynamics in metal NPs has generally been discounted.[14] In this paper, we demonstrate that this difficulty is ameliorated simply by looking at angles other than the illumination direction. To the best of our knowledge, this is the first measurement of diffracted SH from NPs with such a high degree of symmetry.

Recently, it has been proposed that arranging asymmetric NPs in a diffraction grating should provide spatial separation of NP-generated SH light from both the incident fundamental beam and the substrate-generated SH light,[25] a technique demonstrated in the 1980s on asymmetric Ag NPs supported on an array of dielectric posts.[2] (From the constructive interference condition $\sin\theta = m\lambda$, odd-integer orders of the second harmonic are equivalent to half orders of the fundamental, so SH light appears where fundamental light does not. This principle has been used to study SHG from one-dimensional (1D) diffraction gratings of polymers,[26] adsorbed dye molecules,[27] and metals.[28]) However, asymmetric NPs are not strictly necessary. We report diffracted SHG from Au nanorods of planar *symmetry* aligned in a symmetric two-dimensional grating, even when optically excited in a symmetric manner. The resulting SH diffraction pattern is unique in that virtually *no zero-order peak exists*, and the SHG intensity *increases* with diffracted order for a single array (and generally with increasing the angle of observation from the normal). The SHG depends strongly on resonant enhancement between the particle plasmon resonance and the excitation frequency.

Nanorod arrays were fabricated on indium-tin-oxide (ITO)–coated glass by focused-ion-beam lithography (IBL) and thermal evaporation. IBL details may be found elsewhere.[29] Au was evaporated over the polymer mask to 20-nm mass thickness, measured *in situ* with a quartz crystal microbalance, and *ex situ* by a spectrophotometric analysis of a codeposited cover slide. Scanning electron microscopy (SEM) was used to examine array integrity and NP structure (Fig. 1 inset). Minor defects in the IBL process gave rise to regions of irregular particle coverage, but the overall arrays had excellent diffractive properties. We use nanorods instead of nanodisks (which have higher symmetry) because the different axial lengths in a rod give rise to different resonance energies; hence we may probe SHG on- or off-resonance by rotating the array relative to the incident light. It is also technically easier to control the resonance energy through rod length than through disk diameter.

Figure 1 shows the experimental configuration. The NP arrays, typically $60\times60\ \mu m^2$, were illuminated by a passively mode-locked Ti:sapphire resonator pumped by 4.5 W of 532 nm light; the oscillator produces 50-fs pulses with the center wavelength 800 nm at 93 MHz pulse-repetition frequency with an average power ~250 mW. Residual green pump light was blocked with a color filter. Power fluctuations were monitored by a silicon photodiode. Pulse duration

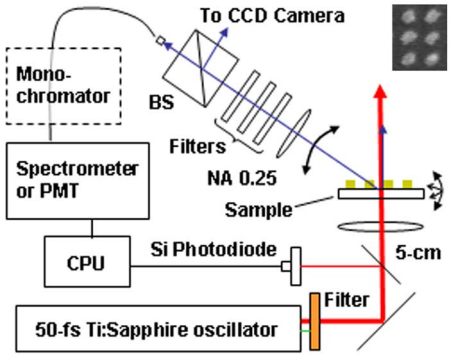

FIG. 1. (Color online). Experimental setup for measuring angular distribution of SH light. Inset: SEM image of "tilted" rods with 200 nm spacing.

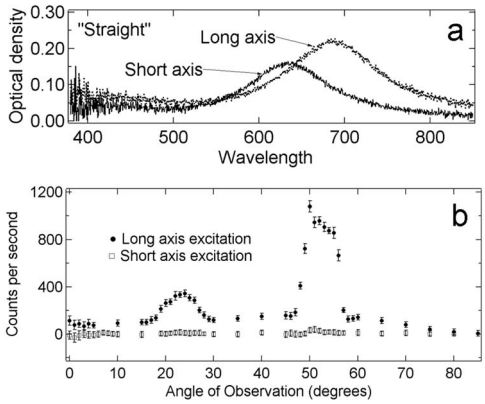

FIG. 2. (a) Polarization-dependent extinction from "straight" rods. (b) Angular distribution of the SHG for the two polarizations. All diffraction patterns are corrected for electrical dark and for the nonlinear response of the bare substrate.

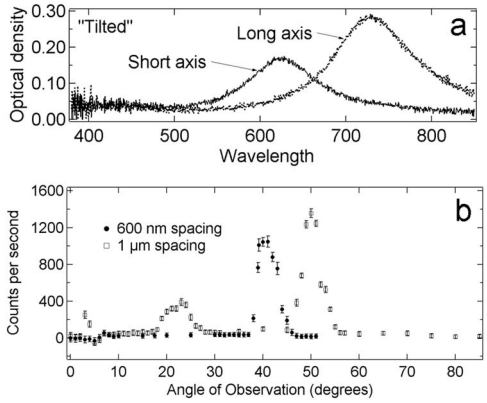

FIG. 3. (a) Polarization-dependent extinction from tilted rods. (b) Angular distribution of the SHG with varying lattice spacing. The signal from the 600-nm-spacing array is scaled by 0.36 to match the areal density of the 1-μm-spacing array.

was measured with an autocorrelator. The fluence was sufficiently low (<0.1 mJ/cm^2) that SHG was achieved without modifying NP morphology. The linear extinction coefficients along the major and minor axes of the nanorods were determined separately with a white-light source and rotatable linear polarizer.

A 5-cm focal length lens focused the fundamental beam to a ~ 50 μm diameter spot. We employed the configuration of Zheludev and Emelýanov,[25] in which the laser is normally incident from the rear of the substrate. The arrays were aligned so that the incident polarization pointed along a grating axis. The nanorods pointed either along the grating axis or at a 45° angle to it. The detector arm rotated in the plane defined by the fundamental propagation and polarization directions.

The detector optical train consisted of a microscope objective (NA 0.25), removable filters, a beamsplitter cube for camera viewing, and an optical fiber to direct the light either to a spectrometer with a Peltier-cooled charge-coupled device array or a photomultiplier tube (PMT) connected to a photon counting module. For PMT measurements, the SH was filtered by a monochromator set to pass 400 nm, assuring the spectral purity of the signal. At each observation angle the PMT signal was optimized; where multiple measurements were acquired at an angle, the highest recorded value is plotted. In the figures, the relative error is plotted, representing the standard deviation of ten consecutive measurements. Due to a difficult alignment the absolute uncertainty could be substantially higher.

A pervasive difficulty in optical spectroscopy of NP arrays is separating the optical signal from the nanorod array from numerous sources of background light. In this case light must be collected from a 60×60 μm^2 area. In the confocal geometry[30] the source (the NP array) is at the focal point of a 10X microscope objective, which refocuses the light to the pinhole of an optical fiber, as in the fiber-optic confocal microscope of Dabbs and Glass.[31] For one-to-one imaging the field of view (FOV) is approximately the same size as the pinhole. We used a 400-μm optical fiber mounted on an adjustable stage as the pinhole, therefore collecting light from a FOV roughly 30 times the area of the NP array. While using a relatively large pinhole that diminished the achievable signal to noise, it provided some flexibility in the alignment.[1–3]

Figure 2 shows the angular distribution of the SH light from a 1-μm grating of Au nanorods aligned along the grating axes. The SH output from the long axis is greatly enhanced relative to the short axis because the linear extinction of the long axis is nearly triple that of the short axis at the excitation wavelength of 800 nm. In the resonant case, the diffracted peak amplitudes are reversed from the conventional situation.

Angular distributions for SH light diffracted by "tilted" rods at NP spacings of 600 nm and 1 μm, respectively, are plotted in Fig. 3. When normalized to NP areal density, patterns from the two arrays display a general trend of an increasing peak intensity with an increasing observation angle. These rods are longer than those of Fig. 2; thus they exhibit greater extinction (in the long-axis mode) than the "straight" rods at the excitation wavelength of 800 nm.[32] This is why, although the particle orientation with respect to the laser is not optimal, the SH output is comparable to the straight-rod case.

At an observation angle of 0°, we observe no SH light except a small and easily identified background that appears in the absence of the arrays. This spurious signal is probably generated at the collection objective by the incident beam, and is generally weaker than the diffracted SH peaks. The first diffracted order of fundamental light is a tiny fraction of the incident beam, so it likely lacks the intensity to produce spurious SH. Thus, even though the second diffracted order of the SH coincides with the first diffracted order of the fundamental, we are confident that we observe only SHG from the NP array at all orders.

The angular distribution in a given measurement is the superposition of the radiation pattern from an individual NP with the diffraction pattern dictated by the array geometry. By adjusting the grating constant, we select the emission angle; in this way we may reproduce the overall angular distribution from the individual nanorods with high sensitivity due to constructive interference. In all cases we observe no forward-scattered SH light from the NPs, as expected

from the symmetry of the array. Several possible mechanisms may give rise to the observed radiation patterns. In the case of isolated centrosymmetric spheres, such a pattern can be produced either by (1) SH dipole emission generated in a nonlocal process involving both volume and surface susceptibilities of the NPs; or (2) SH quadrupole emission in a local process involving only surface susceptibilities.[33] Either mechanism could be effective in our particles. However, in our particular case the rods are supported on a substrate, so the dielectric environment is asymmetric perpendicular to the substrate with air above and ITO below. This configuration could potentially generate SH even without these more complex mechanisms, since there is a nonzero effective second-order susceptibility (due to the broken symmetry) of the form $\chi^{(2)}_{\perp\parallel\parallel}$. Such a mechanism is similar in spirit to so-called electron ratchets, in which geometrical asymmetry causes an applied alternating electric field in one direction to induce direct current in an orthogonal direction.[34] (Of course, in our case we are asserting *alternating* induced motion, so there is no current flow and the NPs are not ratchets at all.) The data presented in Fig. 3 are insufficient to judge whether there is a quadrupolar component to the SH emission pattern; quadrupolar components could be distinguished at angles θ such that $3\cos^2(\theta) > 1$, i.e., at angles beyond 55°.

A simple model of resonant enhancement and SH diffraction gives qualitative agreement with our results. In this model, SH light is generated from an effective dipole SH source which itself varies as the square of the local fundamental field (LFF); thus the SH intensity goes as the fourth power of the LFF, which arises from the response of the ellipsoid to the incident electric field. We caution that this model does not account for multipolar excitations which may indeed be present in particles of the size examined here, and we have further assumed that the induced SH source is purely dipolar and perpendicular to the substrate (i.e., out of plane) without reference to any nonlinear susceptibilities. Still, the main features of the experiment—diffraction and resonant enhancement—are reproduced rather well, indicating that the model incorporates most of the essential physics. In addition, although the particles are ~100 nm in the lateral dimensions (which may give rise to quadrupole effects), their height is only 20 nm; thus for the excitation geometry we used, retardation effects should be small since $h/\lambda \sim \frac{1}{40}$.[35]

The nanorods may be loosely approximated by general ellipsoids. Using a plane wave approximation for the incident light with the foregoing approximations, we may write the induced LFF along an axis of the nanorod (normalized to the incident field) as follows:[32]

$$\frac{E_{1j}}{E_0} = 1 - \left(\frac{L_j}{\varepsilon_1 - 1}\right)\frac{(\varepsilon_1 - \varepsilon_m)^2}{\varepsilon_m + L_j(\varepsilon_1 - \varepsilon_m)},$$

with indices $j = x, y, z$ corresponding to ellipsoid semiaxes $a \geq b \geq c$, respectively. The shape factors L_j may be written as integrals and computed numerically; for example,

$$L_x = \frac{abc}{2}\int_0^\infty \frac{dq}{(a^2+q)\sqrt{(a^2+q)(b^2+q)(c^2+q)}}.$$

It is instructive to note that, for wavelengths near resonance, the ratio between the LFFs for the x and y axes reduces to

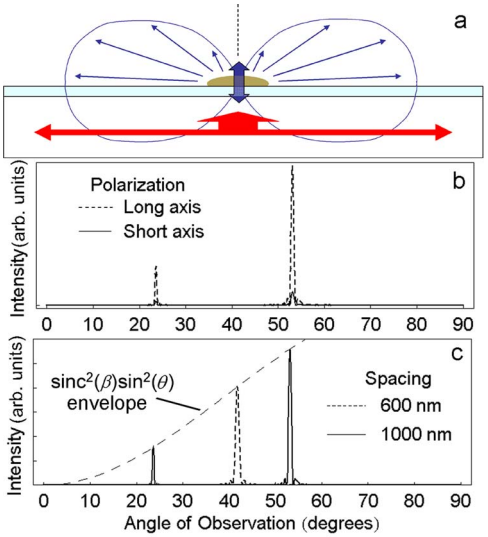

FIG. 4. (Color online) (a) Diagram of the SH dipole emission pattern. (b) Model calculation of 2(b). (c) Model calculation of 3(b).

$$\frac{E_{1x}}{E_{1y}} = \frac{\varepsilon_1 - \varepsilon_m\left(1 - \frac{1}{L_y}\right)}{\varepsilon_1 - \varepsilon_m\left(1 - \frac{1}{L_x}\right)}.$$

When the numerator and denominator of the RHS are set equal to zero, we obtain the surface plasmon resonance condition for general ellipsoids.[32]

Due to the planar fabrication method, the NPs are not strictly ellipsoidal. However, if we assume a fixed particle height $2c = 20$ nm, the extinction maxima of Fig. 2(a) can be approximated by an ellipsoid of dimensions $2a = 90$ nm, $2b = 78$ nm. These parameters were used to calculate the ratio of SH intensities for the major and minor axes, plotted in Fig. 4(a). Assuming a purely dipolar SH radiation pattern varying with angle as sine-squared, we have modeled Figs. 2(b) and 3(b) using the equations[36]

$$I(\theta) \propto \left(\frac{\sin\beta}{N\beta}\right)^2\left(\frac{\sin N\alpha}{\sin\alpha}\right)^2 \sin^2\theta, \quad \alpha \equiv \frac{k\ell_1}{2}\sin\theta,$$

$$\beta \equiv \frac{k\ell_2}{2}\sin\theta,$$

where N is the number of NPs in a row, k is the wave number, and ℓ_1 and ℓ_2 are the grating spacing and NP size, respectively. The results, plotted in Fig. 4, agree reasonably with our experiments. The intrinsic width of the peaks, which is approximately 1°, is not resolved in our experiments due to a relatively large numerical aperture.

The individual particles have considerable substructure common to lithographic NPs, as evidenced by the SEM image. Local field enhancement can be substantial at nanoscale roughness features, giving rise to enhanced nonlinearities, so the roughness defects may be considered SH sources.[37] In addition, deviations from ideal NP shapes have been linked to optical activity particularly in SHG patterns.[38] However, the observed SH diffraction pattern specifies that such defects may not radiate constructively in the forward direction. The data suggest that roughness defects are distributed more or less randomly on the NPs, and our excitation geometry

and detection scheme are insensitive to the tensor components discussed in Ref. 38, so we observe no shape bias. There is a small "noise" SH signal at most angles, as seen in Fig. 2 (especially for the resonant case), which is not attributable to the substrate and is probably due to incomplete cancellation from missing particles rather than the other types of defects.

The SH light from the arrays should retain the temporal coherence properties of the incident light. Our experiment bears a superficial resemblance to hyper-Rayleigh scattering measurements,[5,39] which produce incoherent SH light; however, in the case of arrays the excitation at each particle has a well-defined phase relationship to the others, yielding a coherent output.

The scheme used here differs from that of Ref. 25 in that the NPs we studied have in-plane symmetry. We note that angular measurements on asymmetric particles would retain the out-of-plane SH contribution, while exhibiting an additional in-plane contribution due to individual NP asymmetry. This is not explicitly accounted for in Ref. 25, and could complicate the interpretation of such experiments because the proportion of the out-of-plane contribution would depend on the diffracted angle and hence on the grating spacing. Specifically, the prediction that the ratio of the first-order SH peak to the first-order fundamental peak depends only on the particle structure is called into question. Our experiment demonstrates that SH may be produced and directed by an appropriately designed grating using symmetric particles, avoiding complications in both lithography and interpretation. This has implications for photonics.

We thank L.C. Feldman for helpful discussions. Research at Vanderbilt University was supported by the U.S. Department of Energy, Office of Science, Grant No. DE-FG02-01ER45916. P.H.B. was supported by the National Science Foundation Grant No. DMR-0210785; E.A.R. received support from William Jewell College. Support for the focused-ion-beam nanolithography system was provided by Major Research Instrumentation Grant No. DMR-9871234 from the National Science Foundation, and by the Vanderbilt Academic Venture Capital Fund.

[1] T. Götz, M. Buck, C. Dressler, F. Eisert, and F. Träger, Appl. Phys. A **60**, 607 (1995).
[2] A. Wokaun, J. G. Bergman, J. P. Heritage, A. M. Glass, P. F. Liao, and D. H. Olson, Phys. Rev. B **24**, 849 (1981).
[3] F. R. Aussenegg, A. Leitner, and H. Gold, Appl. Phys. A **60**, 97 (1995).
[4] B. Lamprecht, A. Leitner, and F. R. Aussenegg, Appl. Phys. B **64**, 269 (1997).
[5] E. C. Hao, G. C. Schatz, R. C. Johnson, and J. T. Hupp, J. Chem. Phys. **117**, 5963 (2002).
[6] R. C. Johnson, J. T. Li, J. T. Hupp, and G. C. Schatz, Chem. Phys. Lett. **356**, 534 (2002).
[7] B. K. Canfield, S. Kujalal, K. Jefimovs, T. Vallius, J. Turunen, and M. Kauranen, J. Opt. A, Pure Appl. Opt. **7**, S110 (2005).
[8] A. M. Malvezzi, M. Patrini, A. Stella, P. Tognini, P. Cheyssac, and R. Kofman, Eur. Phys. J. D **16**, 321 (2001).
[9] A. Podlipensky, J. Lange, G. Seifert, H. Graener, and I. Cravetchi, Opt. Lett. **28**, 716 (2003).
[10] Y. R. Shen, *The Principles of Nonlinear Optics* (John Wiley and Sons, New York, 1984).
[11] U. Kreibig and M. Vollmer, *Optical Properties of Metal Clusters* (Springer-Verlag, Berlin-Heidelberg, 1995).
[12] T. Vartanyan, M. Simon, and F. Trager, Appl. Phys. B **68**, 425 (1999).
[13] M. Simon, F. Trager, A. Assion, B. Lang, S. Voll, and G. Gerber, Chem. Phys. Lett. **296**, 579 (1998).
[14] B. Lamprecht, J. R. Krenn, A. Leitner, and F. R. Aussenegg, Phys. Rev. Lett. **83**, 4421 (1999).
[15] B. Lamprecht, J. R. Krenn, A. Leitner, and F. R. Aussenegg, Appl. Phys. B **69**, 223 (1999).
[16] B. Lamprecht, A. Leitner, and F. R. Aussenegg, Appl. Phys. B **68**, 419 (1999).
[17] H. G. Bingler, H. Brunner, A. Leitner, F. R. Aussenegg, and A. Wokaun, Mol. Phys. **85**, 587 (1995).
[18] P. F. Liao, J. G. Bergman, D. S. Chemla, A. Wokaun, J. Melngailis, A. M. Hawryluk, and N. P. Economou, Chem. Phys. Lett. **82**, 355 (1981).
[19] E. Hao and G. C. Schatz, J. Chem. Phys. **120**, 357 (2004).
[20] R. F. Haglund, L. Yang, R. H. Magruder, J. E. Wittig, K. Becker, and R. A. Zuhr, Opt. Lett. **18**, 373 (1993).
[21] B. K. Canfield, S. Kujala, M. Kauranen, K. Jefimovs, T. Vallius, and J. Turunen, Appl. Phys. Lett. **86**, 183109 (2005).
[22] G. Assanto, G. Stegeman, M. Sheikbahae, and E. Vanstryland, Appl. Phys. Lett. **62**, 1323 (1993).
[23] Y. Chiu, U. Rambabu, M. H. Hsu, H. P. D. Shieh, C. Y. Chen, and H. H. Lin, J. Appl. Phys. **94**, 1996 (2003).
[24] T. F. Heinz, in *Nonlinear Surface Electromagnetic Phenomena*, edited by H.-E. Ponath and G. I. Stegeman (North-Holland, Amsterdam, 1991), Vol. 29, p. 353.
[25] N. I. Zheludev and V. I. Emel'yanov, J. Opt. A, Pure Appl. Opt. **6**, 26 (2004).
[26] R. D. Schaller, R. J. Saykally, Y. R. Shen, and F. Lagugne-Labarthet, Opt. Lett. **28**, 1296 (2003).
[27] T. Suzuki and T. F. Heinz, Opt. Lett. **14**, 1201 (1989).
[28] A. C. R. Pipino, R. P. Van Duyne, and G. C. Schatz, Proc. SPIE **2622**, 254 (1995).
[29] M. D. McMahon, R. Lopez, H. M. Meyer, L. C. Feldman, and R. F. Haglund, Appl. Phys. B **80**, 915 (2005).
[30] G. Kino and T. Corle, *Confocal Scanning Optical Microscopy and Related Imaging Systems* (Academic Press, New York, 1996).
[31] T. Dabbs and M. Glass, Appl. Opt. **31**, 3030 (1992).
[32] C. F. Bohren and D. R. Huffman, *Absorption and Scattering of Light by Small Particles* (Wiley-Interscience, New York, 1983).
[33] J. I. Dadap, J. Shan, and T. F. Heinz, J. Opt. Soc. Am. B **21**, 1328 (2004).
[34] A. M. Song, Appl. Phys. A **75**, 229 (2002).
[35] J. Nappa, G. Revillod, I. Russier-Antoine, E. Benichou, C. Jonin, and P. F. Brevet, Phys. Rev. B **71**, 165407 (2005).
[36] E. Hecht, *Optics* (Addison-Wesley, Reading, Massachusetts, 1998).
[37] M. I. Stockman, D. J. Bergman, C. Anceau, S. Brasselet, and J. Zyss, Phys. Rev. Lett. **92**, 057402 (2004).
[38] B. K. Canfield, S. Kujala, K. Jefimovs, J. Turunen, and M. Kauranen, Opt. Express **12**, 5418 (2004).
[39] J. I. Dadap, J. Shan, K. B. Eisenthal, and T. F. Heinz, Phys. Rev. Lett. **83**, 4045 (1999).